Copy

CALCULATION REVIEW FORM

Calculation Number/File: PERY-03Q-302 Revision: 0

Review Method: ☑ Design Review ☐ Alternate Calc ☐ Other _____

Scope (PM)	Item	Review Attribute	Reviewer: D. E. DELWICHE
✓	1	Were the inputs correctly selected and incorporated into the analysis? ☑ Yes ☐ No by/date: DEDelwiche 21Oct03	
✓	2	Are all assumptions necessary to perform the analysis reasonable and adequately described? ☑ Yes ☐ No by/date:	
✓	3	Are the applicable codes, standards, and regulatory documents and requirements, including edition and addenda, properly identified, and are their requirements met? ☑ Yes ☐ No by/date:	
✓	4	Is the output reasonable compared to the inputs? ☑ Yes ☐ No by/date:	
✓	5	Are correct material properties used in the analysis? ☑ Yes ☐ No by/date:	
✓	6	Are the acceptance criteria used in the analysis correct? ☑ Yes ☐ No by/date:	
✓	7	Are calculations numerically correct? ☑ Yes ☐ No by/date:	
✓	8	Are information and analysis results accurately transferred from underlying calculations or documents? ☑ Yes ☐ No by/date:	
✓	9	Are the analysis results complete? ☑ Yes ☐ No by/date:	
✓	10	Are known problems or limitations of the results adequately defined? ☑ Yes ☐ No by/date:	
✓	11	Were computer programs used in the analysis adequately identified, verified, tested, and controlled? ☑ Yes ☐ No by/date:	
✓	12	Is the output of computer programs compatible and reasonable compared with the input? ☑ Yes ☐ No by/date:	
✓	13	Are associated computer files correct, current, and available for archival? ☑ Yes ☐ No by/date:	

Documentation Attached: ☑ Markup ☐ Memo ☐ Other _____

Comments (attach pages if necessary):

MARKUPS ARE ON REVIEW COPY -

Proposed Resolution (Preparer):

Reviewer's comments are incorporated

Reviewer Acceptance*/Date: DEDelwiche 21Oct03

The project manager's approval signature, below, also indicates that all design inputs used in the preparation of the attached calculation, and that are referenced in the attached calculation, were reviewed and approved for use by the PM, or his/hers designee.

Project Manager Approval/Date: MissiAL 10/21/03

*Includes agreement that any computer files are current and available for archival

CALCULATION REVIEW FORM

Calculation Number/File: PERY-032-302 Revision: 0

Review Method: ☑ Design Review ☐ Alternate Calc ☐ Other _____

Scope (PM)	Item	Review Attribute	Reviewer: G.A. MIESSI
✓	1	Were the inputs correctly selected and incorporated into the analysis? ☑ Yes ☐ No by/date: Miessi 10/21/03	
✓	2	Are all assumptions necessary to perform the analysis reasonable and adequately described? ☑ Yes ☐ No by/date: GAM 10/21/03	
✓	3	Are the applicable codes, standards, and regulatory documents and requirements, including edition and addenda, properly identified, and are their requirements met? ☑ Yes ☐ No by/date:	
✓	4	Is the output reasonable compared to the inputs? ☑ Yes ☐ No by/date:	
✓	5	Are correct material properties used in the analysis? ☑ Yes ☐ No by/date:	
✓	6	Are the acceptance criteria used in the analysis correct? ☑ Yes ☐ No by/date:	
✓	7	Are calculations numerically correct? ☑ Yes ☐ No by/date:	
✓	8	Are information and analysis results accurately transferred from underlying calculations or documents? ☑ Yes ☐ No by/date:	
✓	9	Are the analysis results complete? ☑ Yes ☐ No by/date:	
✓	10	Are known problems or limitations of the results adequately defined? ☑ Yes ☐ No by/date:	
✓	11	Were computer programs used in the analysis adequately identified, verified, tested, and controlled? ☑ Yes ☐ No by/date:	
✓	12	Is the output of computer programs compatible and reasonable compared with the input? ☑ Yes ☐ No by/date:	
✓	13	Are associated computer files correct, current, and available for archival? ☑ Yes ☐ No by/date: GAM 10/21/03	

Documentation Attached: ☐ Markup ☐ Memo ☐ Other _____

Comments (attach pages if necessary):

Markups on review copy -

Proposed Resolution (Preparer):

comments incorporated - FHK.

Reviewer Acceptance*/Date: Miessi 10/21/03

The project manager's approval signature, below, also indicates that all design inputs used in the preparation of the attached calculation, and that are referenced in the attached calculation, were reviewed and approved for use by the PM, or his/hers designee.

Project Manager Approval/Date: Miessi 10/21/03

*Includes agreement that any computer files are current and available for archival

STRUCTURAL INTEGRITY Associates	CALCULATION PACKAGE	FILE No.: PERY-03Q-302 PROJECT No.: PERY-03Q

PROJECT NAME: Emergency Service Water System Pump Shaft Coupling Failure Analysis

CLIENT: First Energy Corporation

TITLE: Linear Elastic Fracture Mechanics Evaluation of Cracked Pump Shaft Coupling

Document Revision	Affected Pages	Revision Description	Project Mgr. Approval Signature & Date	Preparer(s) & Checker(s) Signatures & Date
0	1-28 A1-A3 Computer Files	Original Issue	10/21/03	FHK 10/21/03 GAM 10/21/03 DED 10/21/03

Table of Contents

List of Tables

List of Figures

1.0 OBJECTIVE

A coupling failure has been observed for the vertical pump shaft of the emergency service water system at Perry Nuclear Power Plant. The failed coupling was found to be have been vertically misaligned by 1". The objective of this calculation is to perform a linear elastic fracture mechanics evaluation of a cracked pump shaft coupling using finite element method. The calculated stress intensity factors versus crack depth obtained from the finite element analysis are used in a crack growth evaluation of the coupling to more fully understand the dynamics of the coupling failure and to provide recommendations to mitigate possible future failures.

2.0 FINITE ELEMENT ANALYSIS

A finite element model (FEM) for the centered coupling was developed in Reference 1 using the 8-node structural solid (SOLID45) elements of the ANSYS software package [2]. In the previous stress evaluation [1], the peak stresses in the failed off-centered coupling were found to be 35% larger than those in the properly centered coupling. For this linear elastic fracture mechanics evaluation, only the properly centered coupling is considered but the stress intensity factor results can be scaled by 35% for application to the off-centered coupling. It should also be noted that the split rings and set screws are not included in the FEM as they are not expected to contribute to the stresses in the coupling.

In Reference 1, it was concluded that the hoop stress, the main contributor of radial cracking, peaks at the edge of the keyway of the coupling [1]. Therefore, the FEM is modified to incorporate a full length radial flaw along this edge so that the relationship between the stress intensity factor (K) and the crack depth (a) can be determined. In addition, the mesh of the FEM is in the vicinity of the crack is refined for more accuracy in the computation of K. The refined FEM, excluding any modeled cracks, is shown in Figure 1. Similarly, a second model is built to analyze a 1.8 inches long flaw.

In order to model the interface between the different components, non-linear point-to-point contact (CONTAC52) elements are inserted between the contact surfaces between the coupling and the key, and the coupling and the shaft. The contact surfaces between the key and the shaft that are expected to be in compression due to the applied load are merged; this is acceptable as the detailed interaction between the key and the shaft is not the focus of this evaluation.

The tips of the cracks are simulated using singular 20-node structural solid (SOLID95) elements with the mid-side nodes around the crack tip shifted to the quarter point locations. This arrangement can capture the singularity of the crack tips. See Figures 2 through 4 for the locations of the crack tip elements for three of the five evaluated crack depths.

The five evaluated crack depths are: 5%, 10%, 20%, 50%, and 80% of the thickness of the initial ligament (t = 0.3451"). In terms of actual modeled dimensions, the five crack depths are equal to:

0.0175", 0.0350", 0.0700, 0.1570, and 0.2771. This provides a general trend of the *K*s when the crack grows radially through the thickness of the coupling.

3.0 FRACTURE MECHANICS EVALUATION

3.1 Stress Intensity Factor Determination

The models are subjected to the same loads as evaluated in Reference 1. That is, the key is subjected to 42,000 in-lbs of torque, plus a shock factor of 1.1 for torsion [3]. Similar to the finite element model in Reference 1, this load is converted to a force couple and applied at the top end of the upper shaft, while the bottom end of the lower shaft is fixed in order for the load to be appropriately transferred. In addition, one node pair between the key and the coupling and one node pair between the shaft and the coupling are coupled axially near the set screw locations to simulate them (the set screws are not modeled). The top end of the top shaft is held axially to prevent any off-axis rotation.

The resultant stress intensity factor at the crack tips are extracted using built-in fracture mechanics features of ANSYS. The crack tips are sequentially numbered from 101 to 155 along the length of the coupling (see Figure 5). The ANSYS input and output files for the analyses are listed in Appendix A.

3.2 Fracture Toughness

The fracture toughness, K_{Ic}, is the critical value of the stress intensity factor K_I at which brittle fracture is predicted to occur. K_{Ic} can be considered a material constant in a given metallurgical condition and under given conditions of temperature and loading rate. Thus, K_{Ic} can be measured in a laboratory. If the calculated K_I, based on the component geometry, the stress field and crack size, exceeds the fracture toughness, K_{Ic}, then brittle fracture will occur. Explicit values of Type 416 steel, a free-machining grade of Type 410 stainless steel, are not available; however, bounding values may be established based on similar materials. Reference 4 gives an upper bound value of K_{Ic} of 50 ksi$\sqrt{in}$ for Type 410 stainless steel at temperatures between 40°F and 200°F.

The Charpy V-Notch (CVN) impact energy can also be used to estimate K_{Ic}. Rolfe and Barsom [5] include several relationships between K_{Ic} and CVN for materials in the toughness transition temperature region. For example,

$$K_{Ic}^2/E = A(CVN)$$

where, E is the elastic modulus and A is a constant ranging from about 4 to 5. Reference 6 provides CVN data for Type 416 stainless steel material. At 593°F, the CVN is listed at 27 Joules (19.9 ft-lb). Using the expression above with CVN = 19.9 ft-lb., E = 29.0 x 10^6 psi, and A = 4 to 5, the fracture toughness, K_{Ic}, for Type 416 material would be predicted to be in the range of 48 to 54 ksi$\sqrt{in}$. These

values are consistent with the measured values of K_{Ic} reported from Reference 4 cited above. Therefore, a fracture toughness, K_{Ic}, of 50 ksi$\sqrt{in}$ is assumed in this evaluation.

3.3 Crack Growth Evaluation

3.3.1 Material Test and Failure Examination Results

The Perry emergency service water (ESW) pump "A" shaft coupling sleeve was fabricated from Type 416 stainless steel in compliance with ASTM Specification A582. The examination of the failed pump shaft coupling was documented in Reference 7. The pump had approximately 9,000 hours (9,140 hours per Reference 8) of intermittent operation in an ambient temperature environment of pH 8.0-8.5 lake water containing 1-30 ppm chloride, 25-50 ppm sulfate. In addition, the ESW pump is chlorinated with 10-12% solution of sodium hypochlorite for one hour per month. Per Reference 8, ESW Pump "A" had experienced approximately 400 starts since it was rebuilt in July 1997.

Evaluation of the failed coupling [7] resulted in the following reported conclusions:

- The material chemical composition was found to meet the requirements of A582-92 martensite stainless steel
- Hardness values correspond to a typical hardened and tempered condition (approximately 1,000°F) for Type 416 stainless steel
- Micro-hardness measurements (Knoop, 500gm load) found values in the range of HRC to 30. (Bulk Rockwell hardness tests were found to be in the range of 27-28 HRC.)

The failed Perry sleeve has the following composition in comparison to A582 Type 416

	C	Mn	P	S	Si	Cr	Ni	Mo	Cu	Al	Ti
Perry	0.113	0.672	<0.008	0.2589	0.542	13.48	0.232	<0.030	<0.065	<0.008	<0.004
A582 Type 416	0.15 max	1.25 max	0.06 max	0.15 min	1.00 max	12.00 – 14.00	NS	NS	NS	NS	NS

The chemical analysis of scrapped internal deposits/corrosion products showed the following:

- 3.54 ppm Cl (exposed non failed sleeves deposits)
- 1,450 ppm sulfur (failed sleeve ID deposits)

Clearly, the failed sleeve environment has significant levels of chloride, and sulfur, presumably due to continuous lake water exposure and monthly exposure to 10-12% solution of sodium hypochlorite.

The expected performance of Type 416 relative to SCC and fatigue initiation and propagation in ambient temperature lake water environments was evaluated based on documented open-literature materials properties data.

3.3.2 Stress Corrosion Crack Growth

Type 416 stainless steel (A582-92-Type 416) is a free machining modification of Type 410 stainless steel, a heat treatable martensitic type stainless steel. As shown in Reference 9, martensitic Types 403 (same nominal properties as Type 410), 410, and 416 are grouped together in terms of response to annealing, hardening, and tempering. The Perry sleeve was found to have an upper bound Rockwell hardness of 30 R_C, which corresponds to a Brinell hardness value of approximately 287. Reference 10 provides a correlation between hardness (HB) and tempering temperature. This figure indicates the Perry sleeve was tempered at approximately 550°C (1022°F).

Reference 11 provides the effect of tempering temperature and stress intensity on the velocity of stress corrosion cracks in a 12Cr steel as shown in Figure 6. The 12% Cr, 0.2% Carbon Steel, in this context, is categorized along with the Types 403, 410, and 416 Stainless Steels, with nominal Cr content specified to be in the range of 11.5 to 13.5 wt. percent Cr., and the Carbon in the 0.15 to 0.2% range. These steels are iron-chromium steels, martensitic in structure, with or without small additions of other alloying elements. Desired engineering properties are obtained by rapid cooling in air or a liquid medium from above the critical temperature followed by heating the steel to an intermediate temperature. The "general purpose" standard martensitic stainless steel is Type 410, with a nominal Cr content specified at 11.5 to 13.5 percent. The generic categorization is 12 Cr steel. By contrast, a low carbon 12% Cr, 0.08% Carbon steel is a ferritic stainless steel, of the Type 405 family (with nominal properties approximately the same as those of Type 410 in the annealed condition).

The curve shown in Figure 6 indicates a K_{ISCC} of 17 $MN \cdot m^{-3/2}$ (15.5 $ksi\sqrt{in}$), which is fairly independent of tempering temperature, and an upper bound crack velocity curve (for a tempering temperature of 450°C (842°F)) in an ambient temperature distilled water environment. SCC growth rates for lower hardness 416 stainless steel (resulting from a tempering temperature higher than 450°C) would be expected to be lower. Therefore, the lower bound curve in Figure 6 is appropriate for use in this evaluation.

3.3.3 Fatigue Crack Growth

Martensitic stainless steel Types 403, 410, and 416 (A582-92-Type-416) have equivalent microstructures and behavior in terms of annealing, hardening, and tempering. Likewise, the mechanical properties are comparable.

Figure 7, obtained from Reference 12, provides near-threshold fatigue crack growth rates for Type 403 stainless steel obtained in NaCl / Na_2SO_4 solutions. It is noted that the environment (NaCl ranging

from 0.1 g/100ml H_20 to 10 g/100 ml H_20, and Na_2SO_4 ranging from 0.1 to 10.0 g/100 ml H_20, and pH levels ranging from 5.0 to 10.0), has no measurable effect on fatigue crack growth rates. Figure 7, which covers the stress intensity factor ranges, ΔK, below 8 ksi$\sqrt{in}$, also shows that the threshold for fatigue crack growth in Type 403 stainless is approximately 1.5 ksi$\sqrt{in}$. Fatigue crack growth rates at higher stress intensity factor ranges are provided by Reference 13 and presented in Figure 8. As in Figure 7, it is shown in Figure 8 that the pH level has a negligible effect on the fatigue crack growth rate of Type 403 stainless steel. However, the water environment is shown to substantially speed the crack growth rate when compared to air. Also, it is seen that higher temperatures tend to increase the crack growth rate. Since the pump shaft operating temperature is about 80°F, the fatigue crack growth curve for Type 403 stainless steel exposed to 25°C (77°F) water is selected for this evaluation. That curve and the curve from Figure 7 are digitized and the data is curve-fitted in a spreadsheet into a power law equation in the form of a Paris law as:

$$da/dN = C(\Delta K_I)^n$$

where:

	a	=	flaw depth
	N	=	number of stress cycles
C and n		=	experimentally determined parameters related to the material and operating environment
	ΔK_I	=	stress intensity factor range (K_{max} - K_{min})

The resulting fatigue crack growth curves and corresponding equations used in this evaluation are shown in Figure 9.

4.0 RESULTS AND DISCUSSION

4.1 Stress Intensity Factor Results

The deformed shapes of the flawed coupling for the full length axial flaw are shown in Figures 10 through 12 for three of the five analyzed crack depths. The *K*s along the length of each cracked coupling is plotted in Figure 13. The maximum K (K_{max}) for each crack depth (a) is tabulated in Table 4-1. The relationship between the stress intensity factor, K_{max}, and the crack size, a, is plotted and curve fitted in Excel spreadsheet K_Perry.xls and presented in Figure 14; the equation of the curve fit is determined to be:

$$K = 4579.33a^3 - 1630.54a^2 + 246.52a + 28.32 \text{ ksi}\sqrt{\text{in}}$$

The K_{max} versus a for the case of a 1.8 inches long flaw is also shown in Figure 14. It can be seen that the maximum stress intensity factors remain approximately the same in the two cases. This is expected since K_{max} is obtained at the edge of the coupling where the peak hoop stresses are very localized.

In the case of an improperly installed (i.e., off-centered) pump shaft coupling, the stress intensity factor curves can be determined by conservatively scaling the properly centered K_{max} versus a curve upward by 35% as shown in Figure 14.

4.2 Crack Initiation

Type 416 stainless steel is a martensitic stainless steel and is relatively resistant to the environmental effects of chlorides (and the monthly chlorination procedure used at Perry) on crack formation and growth. However, high chloride levels would promote pitting, especially within the crevice regions of the keyway of the coupling. SCC initiation and growth would preferentially occur at pit locations.

The pump shaft failure scenario at Perry is believed to have resulted from SCC crack initiation and growth occurring at pits within the creviced keyway of the coupling. The time to initiation is not well defined. Growth of pitting to sufficient size to promote SCC initiation and growth is dependent upon crevice size and tightness, and the concentration of the hypochlorite treatment solution within the crevice as well as the time required for the crevice environment conditions to return to bulk environment levels.

4.3 Crack Growth Evaluation Results

4.2.1 Stress Corrosion Crack Growth Results

As shown in Figure 11, stress corrosion crack growth is very rapid for A582-92 Type 416 martensitic stainless steel. Using the lower bound curve for 550°C tempering temperature, the SCC growth rate is equal to 2.27×10^{-4} in/hour. This crack growth rate is nearly constant and independent of the range of stress intensity factors. Thus, from the onset of SCC, it is predicted that a flaw could grow to 0.227

inches in 1000 hours, 0.345 inches in 1520 hours and, 2.075 inches in 9,140 hours. Although the effective crack tip stress intensity factor is lower due to the multi-branched nature of SCC crack propagation, it is valid to conclude that, from the onset, SCC growth is rapid. Thus, through-section penetration would be expected within a single plant fuel cycle, once initiation has occurred.

4.2.2 Fatigue Crack Growth Results

The fatigue crack growth analysis is performed using the fracture mechanics computer program pc-CRACK™ [14] and the fatigue crack growth curves derived in Section 3.3.3 with the stress intensity factors shown in Section 4.1. A number of postulated initial flaw sizes are evaluated in order to determine the effect of fatigue on the coupling. The results of the fatigue crack growth analysis are summarized in Table 2 and illustrated in Figure 15 for a sample of postulated initial flaw depths in the two configurations of the coupling under consideration.

A postulated initial crack 0.001 inches deep in the properly centered coupling is predicted to grow 0.0022 to a depth of 0.0032 inches after 400 starts of the ESW pump and, such a crack is predicted to lead to failure of the coupling (i.e., reach 0.2 inches) after 11000 cycles (i.e., pump starts). Similarly, a postulated initial crack 0.01 inches deep (10 times larger than the 1 mil crack) is predicted to grow 0.0053 to a depth of 0.0153 inches after 400 starts of the ESW pump and, lead to failure of the coupling after 9900 cycles and a 0.1 inches deep could grow to a depth of 0.1076 inches after 400 starts of the ESW pump and, lead to failure of the coupling after 4400 cycles.

In comparison, a 0.001 inches deep initial flaw in an improperly installed coupling grows to a depth of 0.0049 inches after 400 pump starts and is predicted to reach the critical crack size after 2580 cycles. And, even for a postulated 0.01" deep flaw, 1900 cycles are needed for the critical flaw to be reached. Thus, fatigue crack growth appears to be very slow in comparison to stress corrosion cracking and, based on the recorded number of starts experienced by the pump, even a flaw as deep as 0.01 inches could not have led to failure solely by the fatigue mechanism.

5.0 CONCLUSION AND RECOMMENDATIONS

The fracture mechanics analyses for the pump shaft coupling show that the maximum stress intensity factors at a postulated axial flaw in the keyway are high, varying from 32 ksi$\sqrt{in}$ for a 0.02 inches deep to 68 ksi$\sqrt{in}$ for a 0.277 inches deep flaw.

The fracture toughness of the coupling material (A582-92 Type 416) is less than 50 ksi$\sqrt{in}$, which corresponds to a flaw depth of 0.2 inches (~60% of radial wall thickness at the keyway groove) for the properly centered coupling. However, for the improperly installed coupling, the critical flaw depth decreases to only 0.05 inches due to the 35% increase in stresses. Thus, in such a case, there is a greater potential for failure by brittle crack propagation.

Stress corrosion cracking in martensitic stainless steel Type 416 proceeds at very high velocities. Using even the lower bound SCC crack growth curve, SCC flaws are predicted to lead to failure in less than 1,520 hours.

Based on the low number of starts (400) that the subject ESW pump has experienced, the fatigue analysis demonstrates that even a relatively large flaw (0.01 inches deep and full axial length) in the coupling would need at least 1900 cycles in the worst case (improperly centered coupling) to lead to failure due to fatigue crack propagation. Hence, failure due to fatigue crack growth is less probable.

The results of the fracture mechanics evaluation suggest that the most significant parameters in the prevention of further failure of the pump shaft coupling are the time to SCC initiation and the stress level at the keyway groove. Therefore, the following recommendations are made:

→ A more SCC resistant material such as 17-4 PH, H1100 should be used to fabricate the pump shaft couplings. It is also noted that the SCC crack velocity behavior shown in Figure 11 exhibits considerable variability with respect to tempering temperature. Recognizing the pronounced effect of heat treatment in the 400 series stainless steel, the ASM Metals Handbook [15] has a note specific to tempering of the 400 series stainless steel; "...Tempering in the range of 700°F (370°C) to 1050°F (565°C) is not recommended. [The Perry coupling sleeve was tempered at approximately 550°C (1022°F)] because it results in low and erratic impact properties and poor resistance to corrosion and stress corrosion." Hence, if Type 416 were to be used, tempering above 1100°F (590°C) would be recommended.

→ The local stress levels in the keyway could be lowered by specifying a reasonable fillet radius for the keyway groove in order to minimize the stress concentration. For example, for the design of keyway in shafts, an approximate fillet radius(r) to shaft diameter (d) ratio r/d = 1/48 is recommended for shaft diameters up to 6.5 inches [16]. Such a proportion can be applicable for the design of the coupling keyway. In addition, proper installation of the keyway will

prevent the 35% increase in the peak stresses at the keyway, which would severely impact the propensity of cracking in the coupling.

6.0 REFERENCES

1. SI Calculation Package PERY-03Q-301, Rev. 0, "Stress Comparison Between a Properly Centered Coupling and an Off-Centered Coupling."
2. ANSYS/Mechanical, Release 6.1 (w/ Service Packs 2 and 3), ANSYS Inc., April 2002.
3. McDonald Engineering Report No. ME-454 (Dated 07/20/1982), "Seismic Analysis of Vertical Pump," Including Addendum No. 1 (Dated 04/03/1984), SI File No. PERY-03Q-201.
4. EPRI Report NP-5511, "Fracture Toughness Characterization of Type 410 Stainless Steel", November 1987.
5. S. T. Rolfe and J. M. Barsom, Fracture and Fatigue Control in Structures, 2nd Edition, Prentice-Hall, NJ, 1987.
6. Materials Reference Data Sheets from BodyCote Materials Testing, "Stainless Steel – Grade 416", www.azom.com.
7. BETA Laboratory Report No. M-03284 Preliminary, "Failure Analysis Report," Dated 09/03/2003, SI File No. PERY-03Q-201.
8. E-Mail and Accompanying Attachments from Jeo Paskar (First Energy) to A. Miessi (SI), "ESW "A" Pump Coupling Reports," Dated 09/23/2003, SI File No. PERY-03Q-202.
9. ASM Metals Handbook, Vol. 1, Tenth Edition, Page 858, Figure 5.
10. ASM Metals Handbook, Vol. 1, Tenth Edition, Page 859, Figure 6.
11. Markus O. Speidel, "Corrosion Fatigue in Fe-Ni-Cr Alloys" published in "Stress Corrosion Cracking and Hydrogen Embrittlement of Iron Base Alloys", NACE-5, National Association of Corrosion Engineers, 1977.
12. ASM Metals Handbook, Vol. 8, Ninth Edition, Page 430.
13. American Society for Metals, "Atlas of Fatigue Curves", Edited by Howard E. Boyer, 1986.
14. **pc-CRACK** for Windows, Version 3.1-98348, Structural Integrity Associates, 1998.
15. Metals Handbook, 8th Edition, Vol. 2, pp 245, Note d.
16. R. E. Peterson, "Stress Concentration Factors", John Wiley & Sons, Inc.,1974.

Table 1: Maximum *K* versus *a* Results

Percentage Through-Wall	Depth, *a* (in)	K_{max} (ksi$\sqrt{in}$)
5%	0.0175	32.117
10%	0.0350	35.061
20%	0.0700	39.078
50%	0.1571	45.835
80%	0.2771	68.462

Table 2: Fatigue Crack Growth Results

Initial Flaw Size (in)	Flaw Size After 400 Cycles [1]		Allowable Number of Cycles [2]	
	Centered	Off-Centered	Centered	Off-Centered
0.001	0.0032	0.0049	11000	2580
0.005	0.0099	0.0124	10300	2180
0.01	0.0153	0.0179	9900	1900
0.05	0.0566	---[3]	7200	---[3]
0.1	0.1076	---[3]	4400	---[3]

1. A cycle is equivalent to a pump start.
2. Number of cycles necessary to exceed the fracture toughness of 50 ksi$\sqrt{in}$ and reach the critical flaw depth (0.2" and 0.05" for centered and off-centered couplings, respectively).
3. Flaw depth is equal or exceeds the critical flaw depth of 0.05" for off-centered coupling.

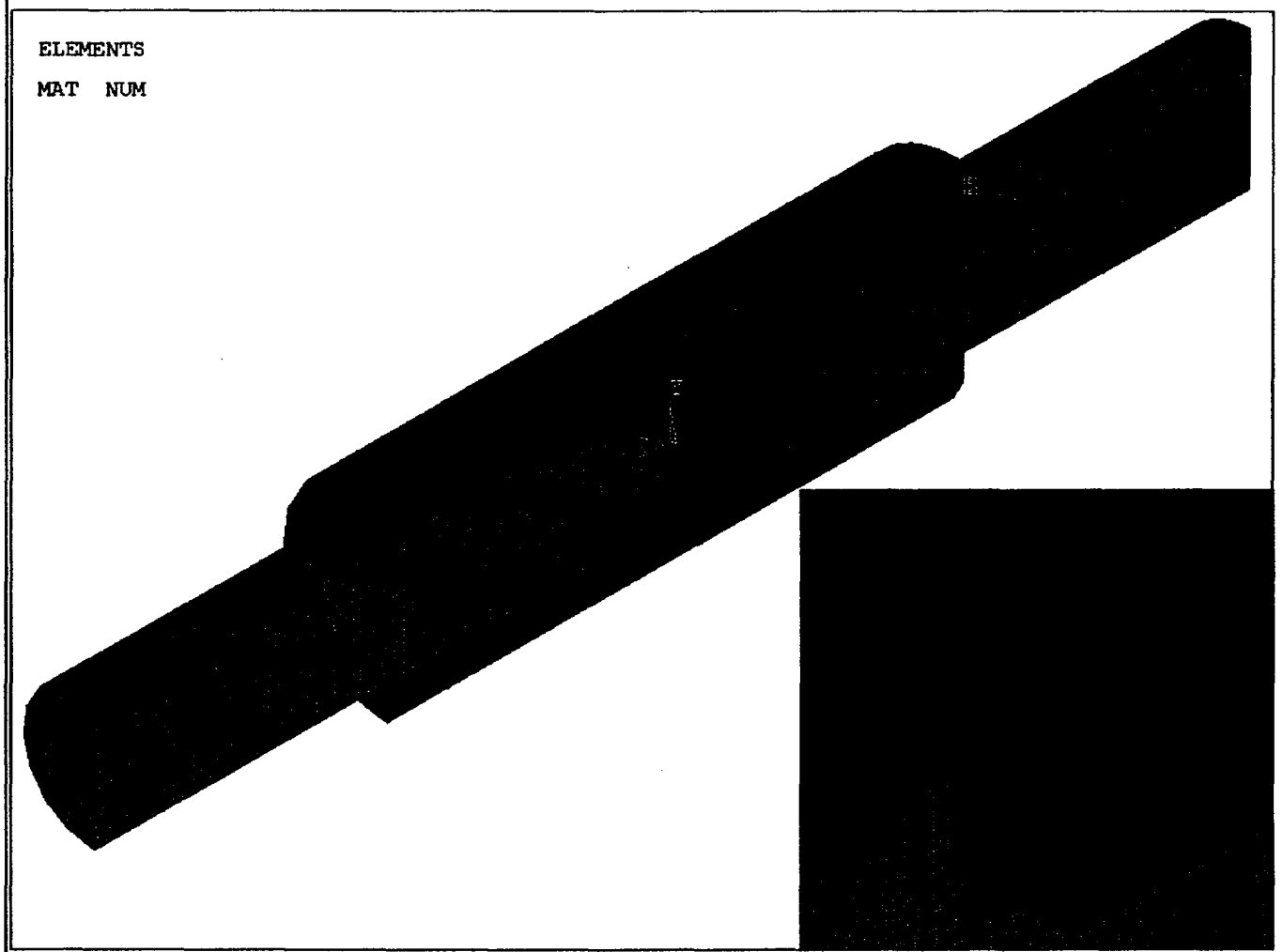

Figure 1: Isometric View of the Refined Finite Element Model

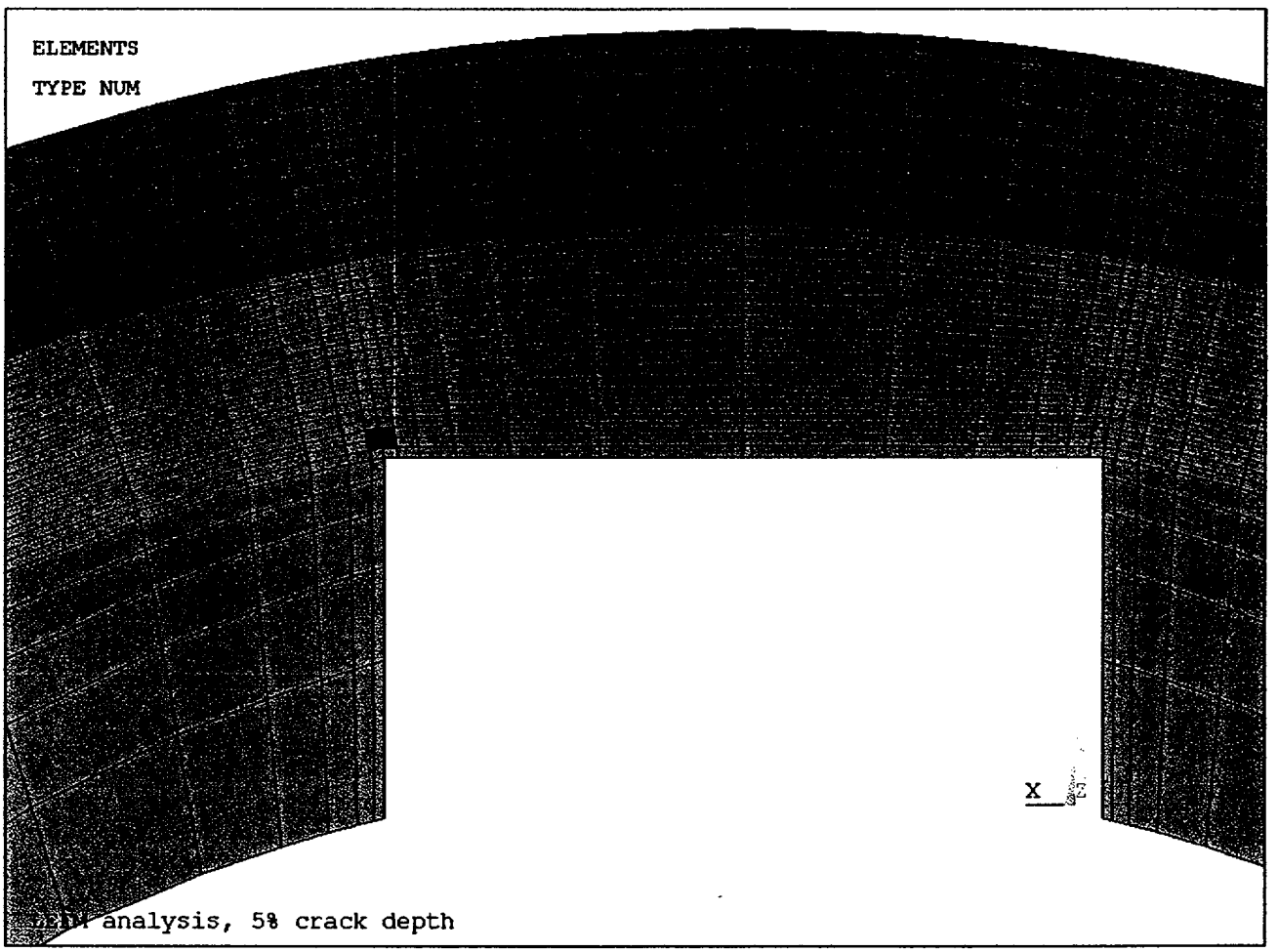

Figure 2: Modeled 5% Crack Depth

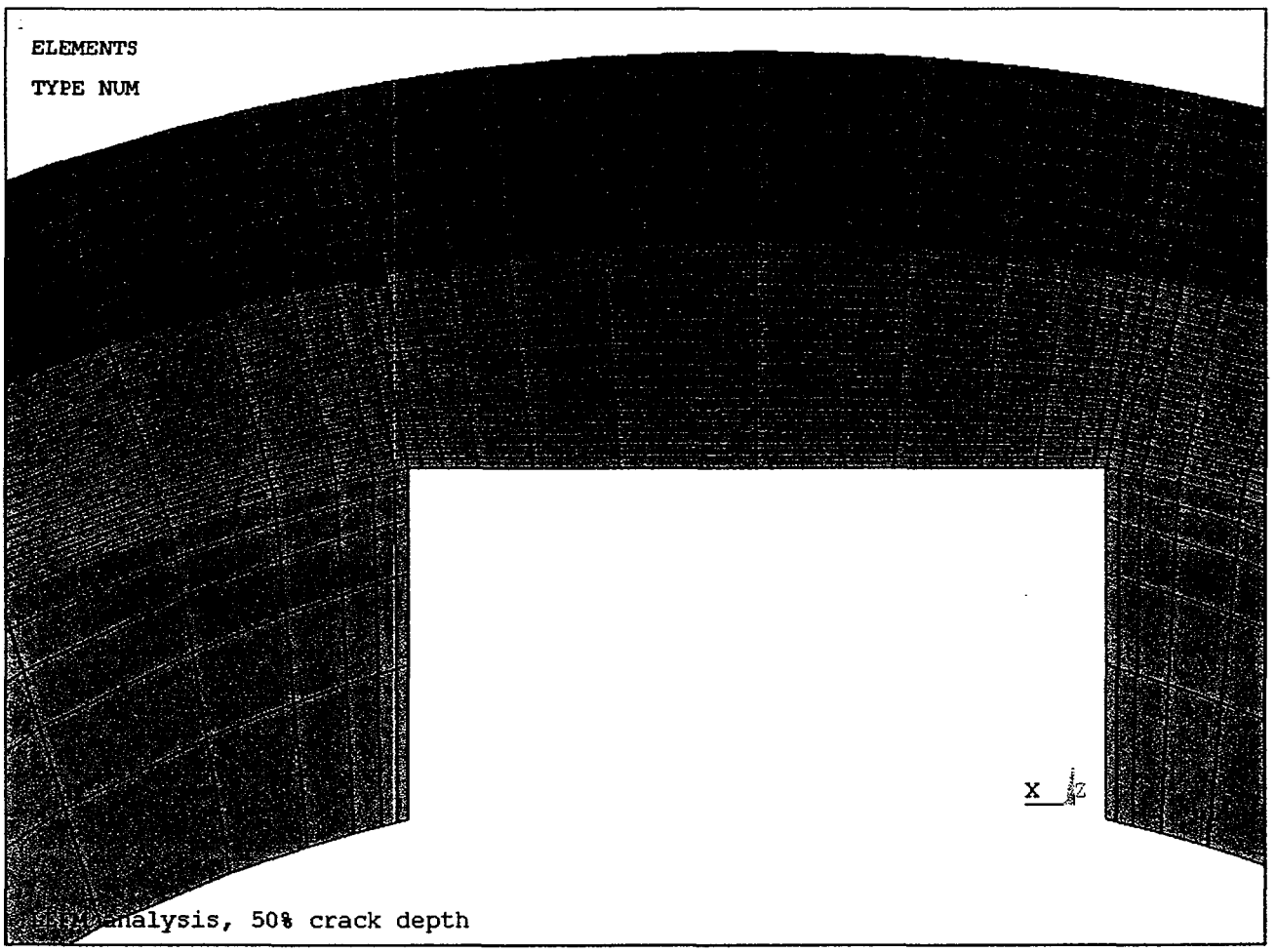

Figure 3: Modeled 50% Crack Depth

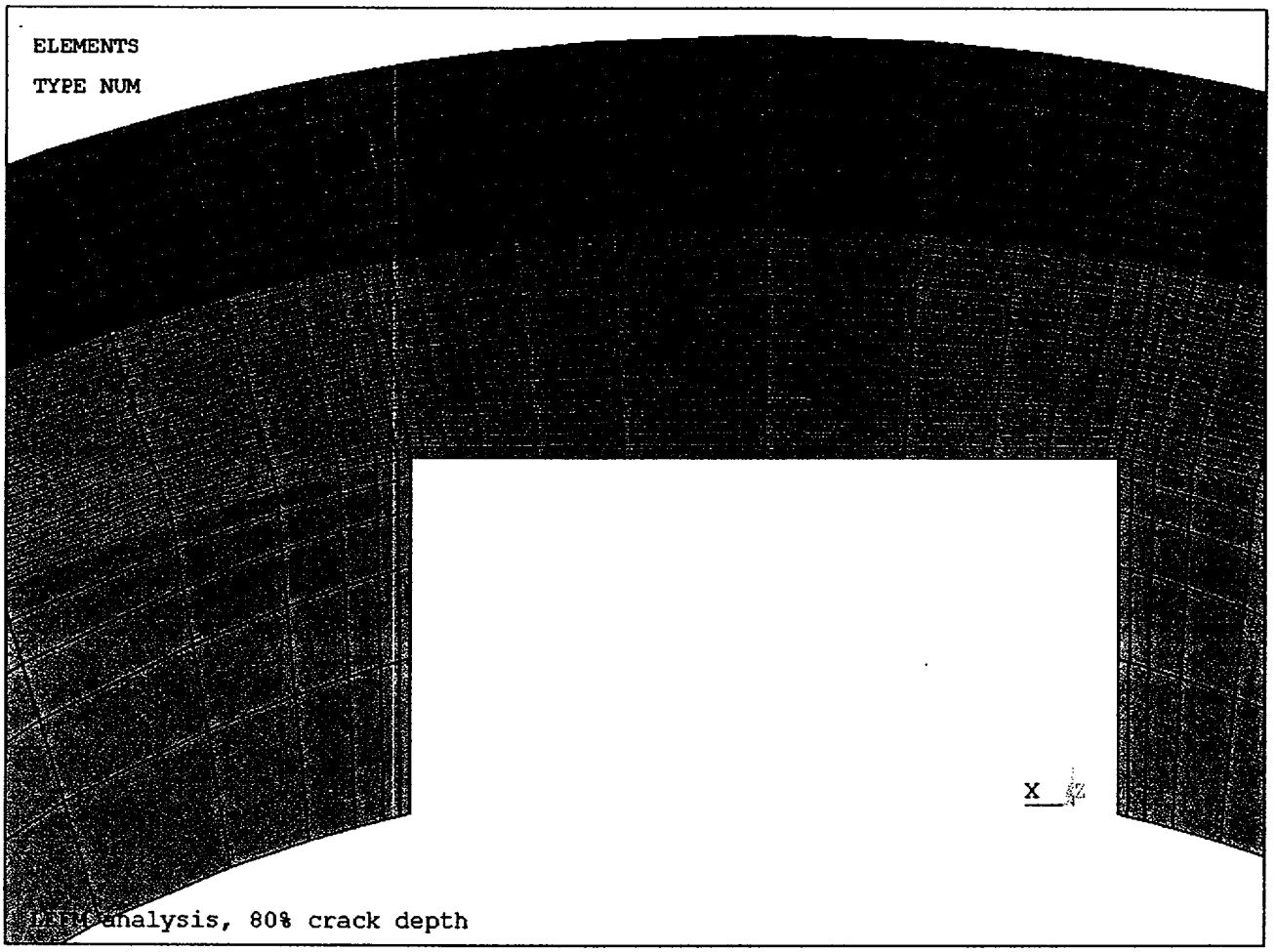

Figure 4: Modeled 80% Crack Depth

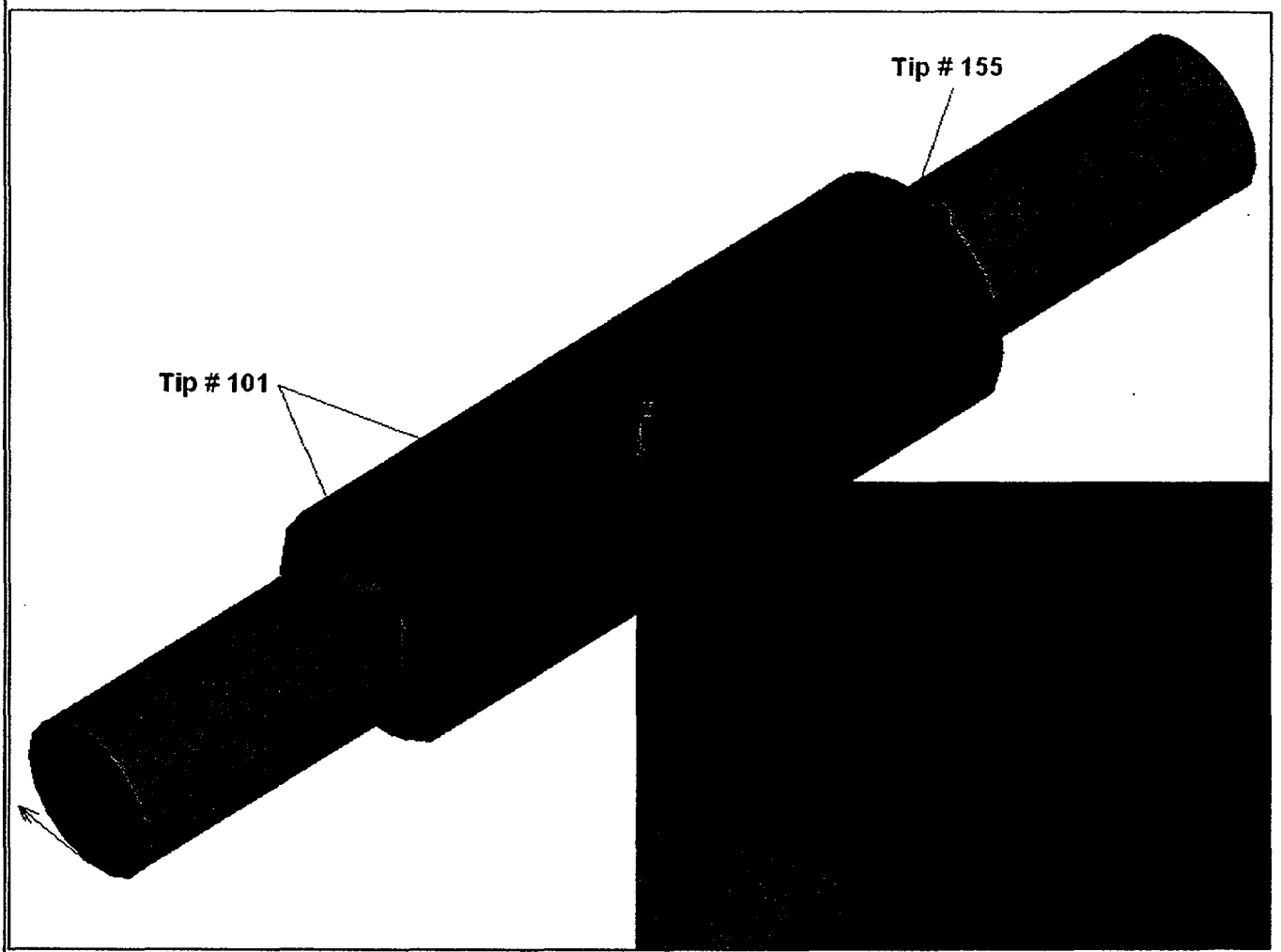

Figure 5: Crack Tip Numbering

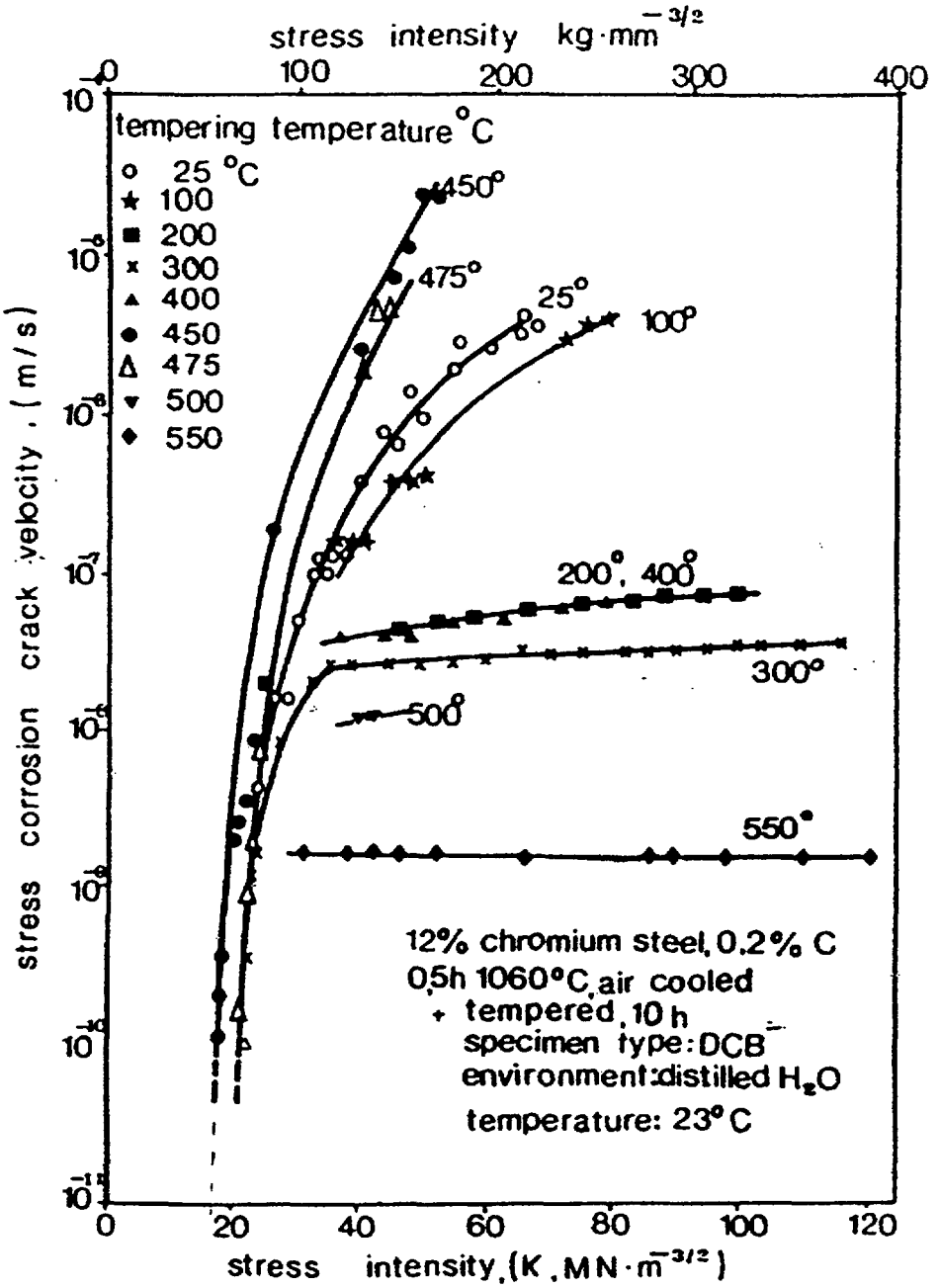

Figure 6: Effect of Tempering Temperature and Stress Intensity on the Velocity of Stress-Corrosion Cracks in a 12Cr Steel [5]

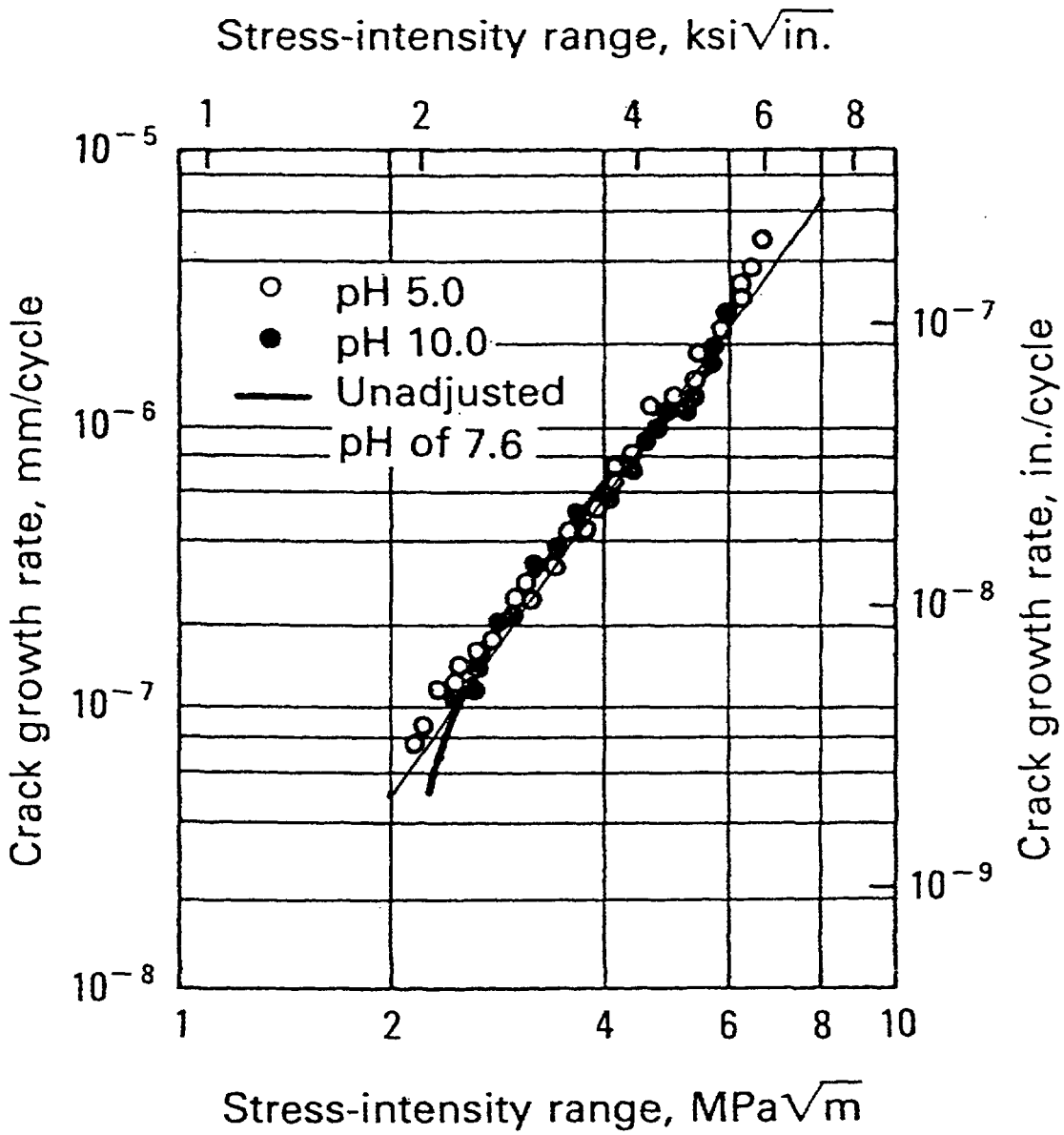

Figure 7: Effect of pH on Near-Threshold Fatigue Crack Growth Rates in Type 403 Stainless Steel

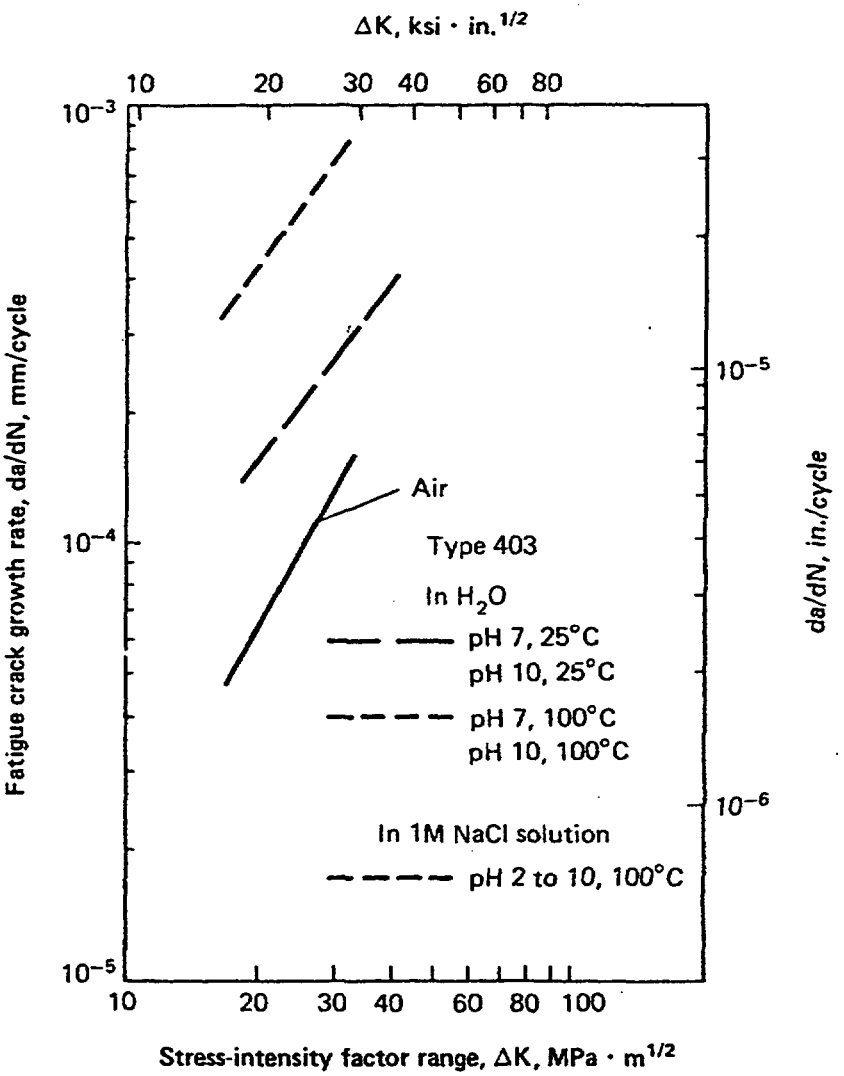

Figure 8: Fatigue Crack Growth Rates in Type 403 Stainless Steel in Air, Water, and a 1M NaCl Solution at 10 Hz and an R ratio of 0.5

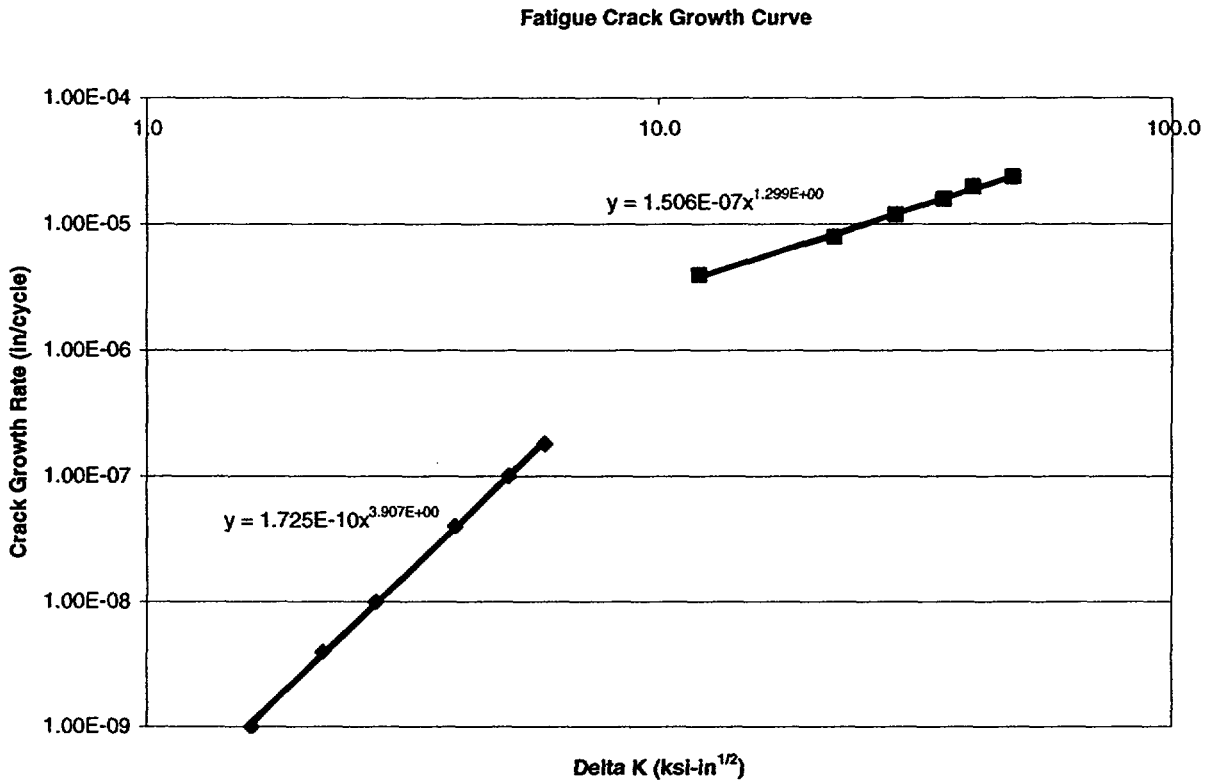

Figure 9: Curve-Fitted Fatigue Crack Growth Rates

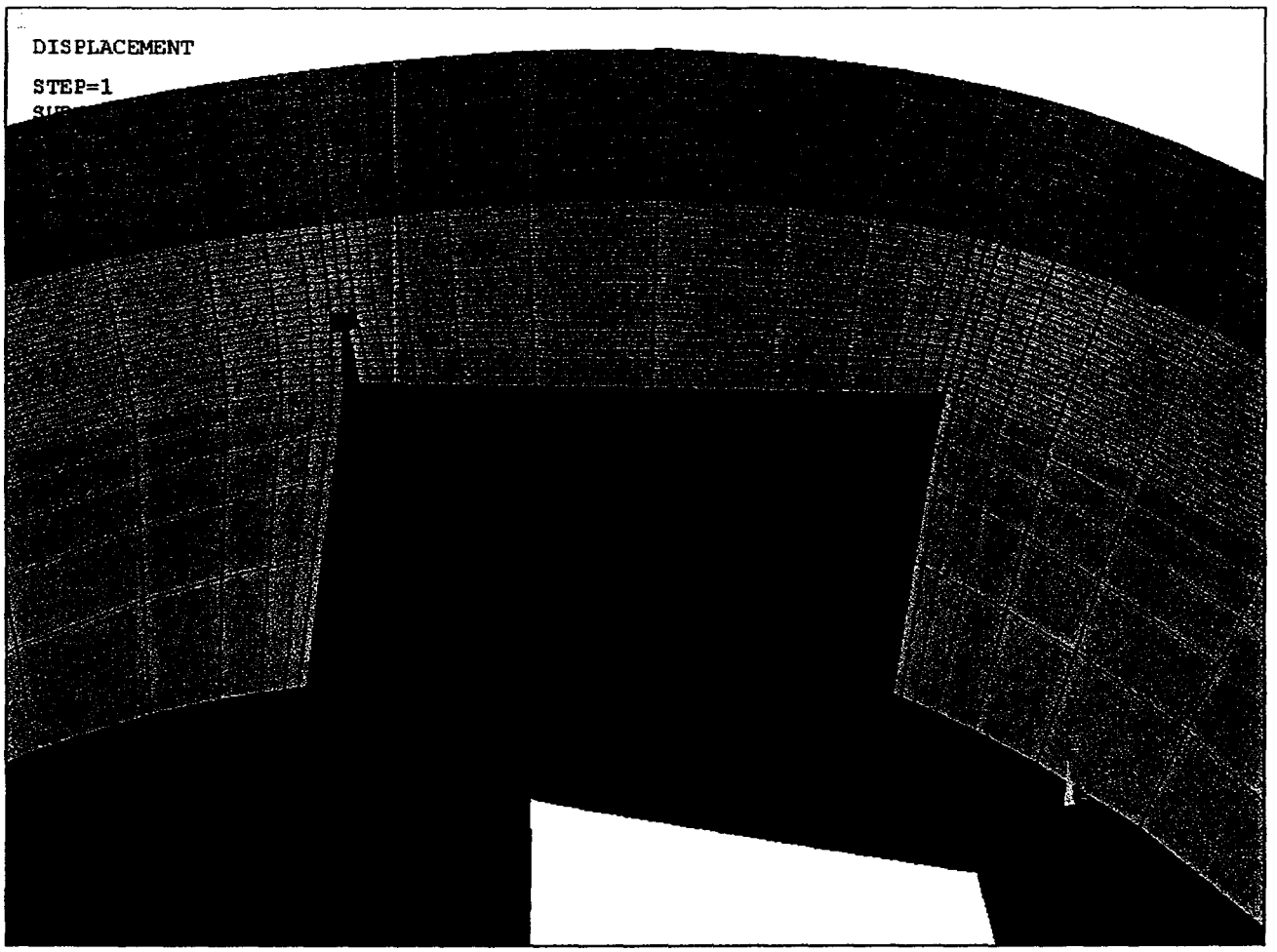

Figure 10: Deformed Shape of the 20% Crack

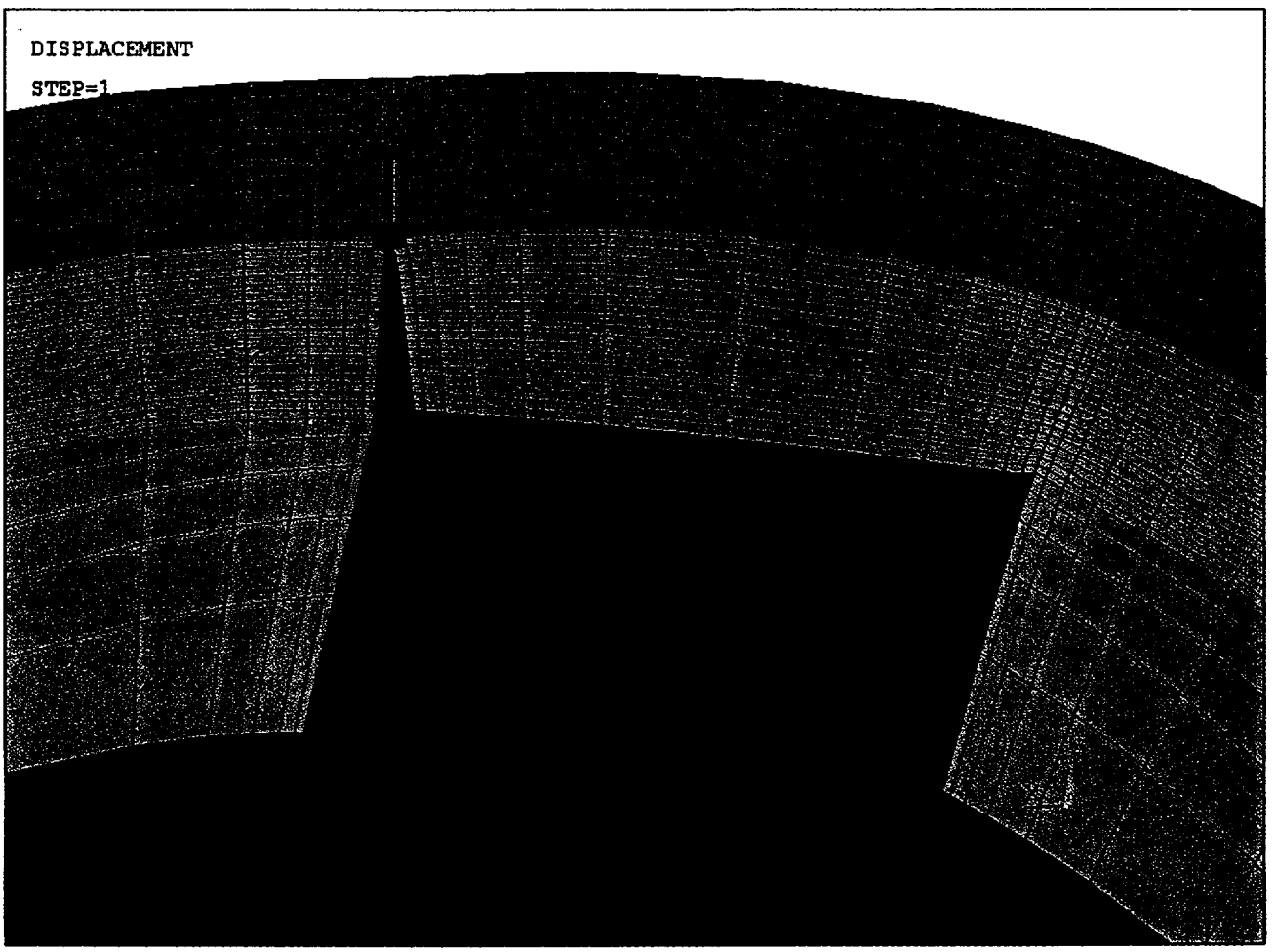

Figure 11: Deformed Shape of the 50% Crack

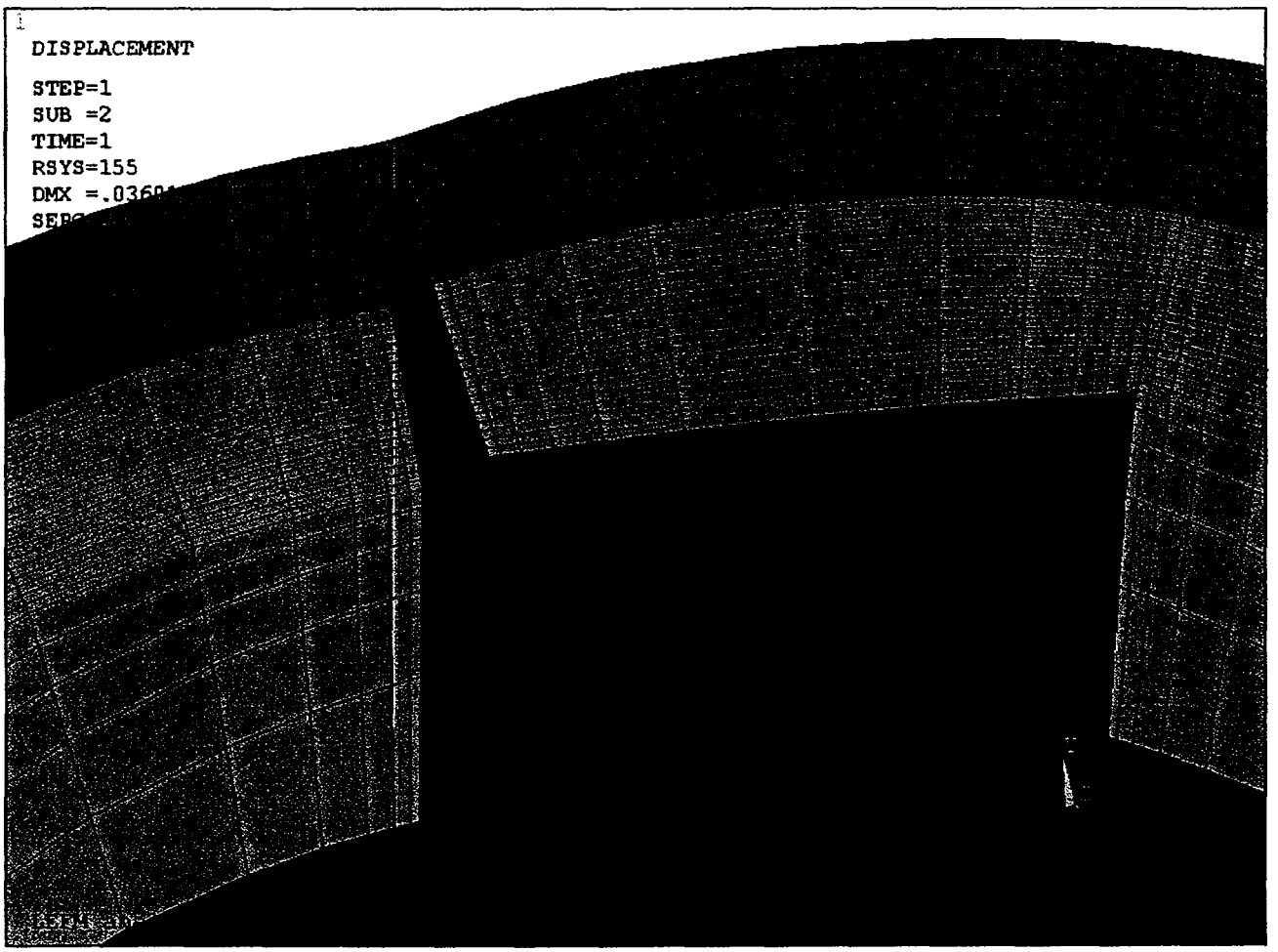

Figure 12: Deformed Shape of the 80% Crack

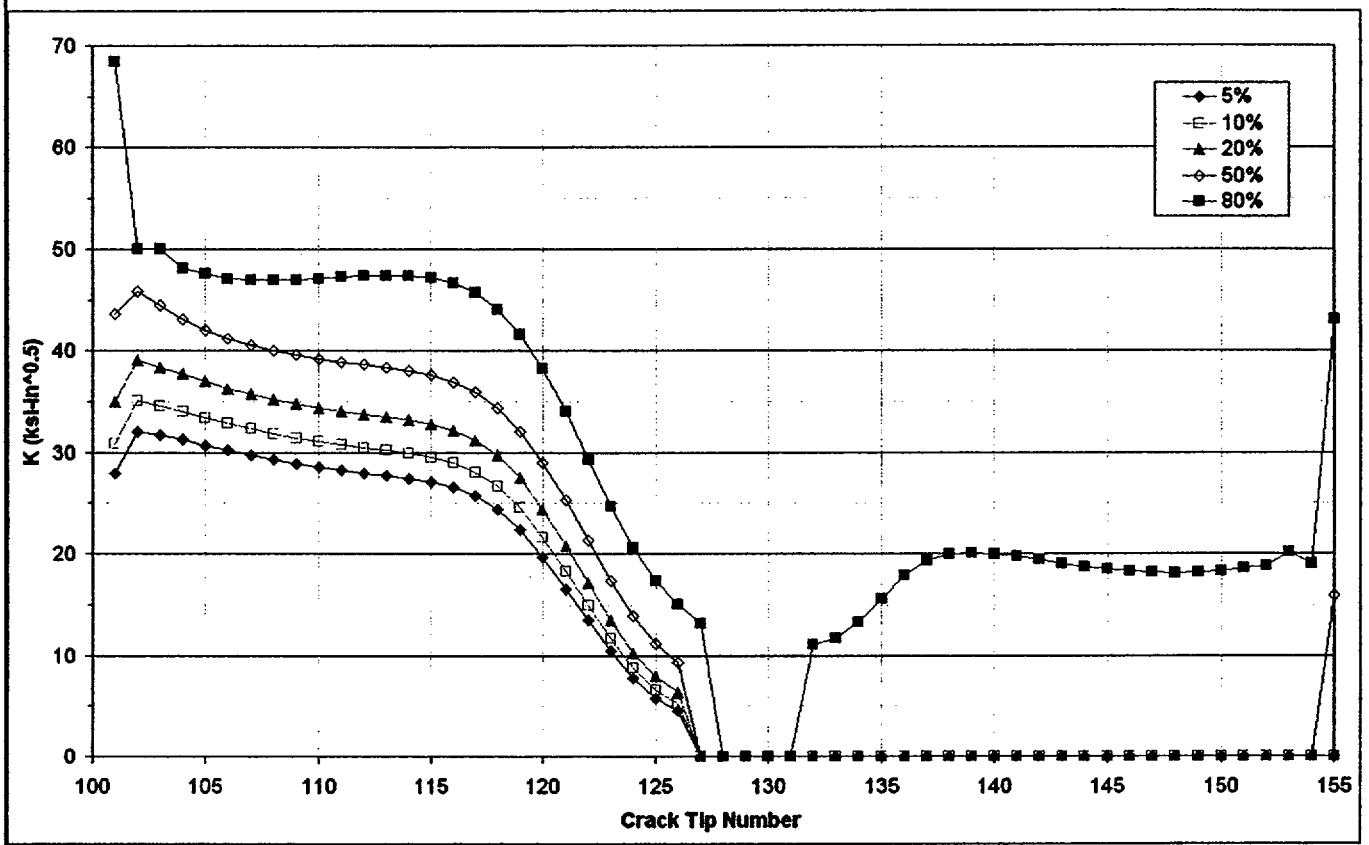

Figure 13: *K* Variations for Various Crack Depths

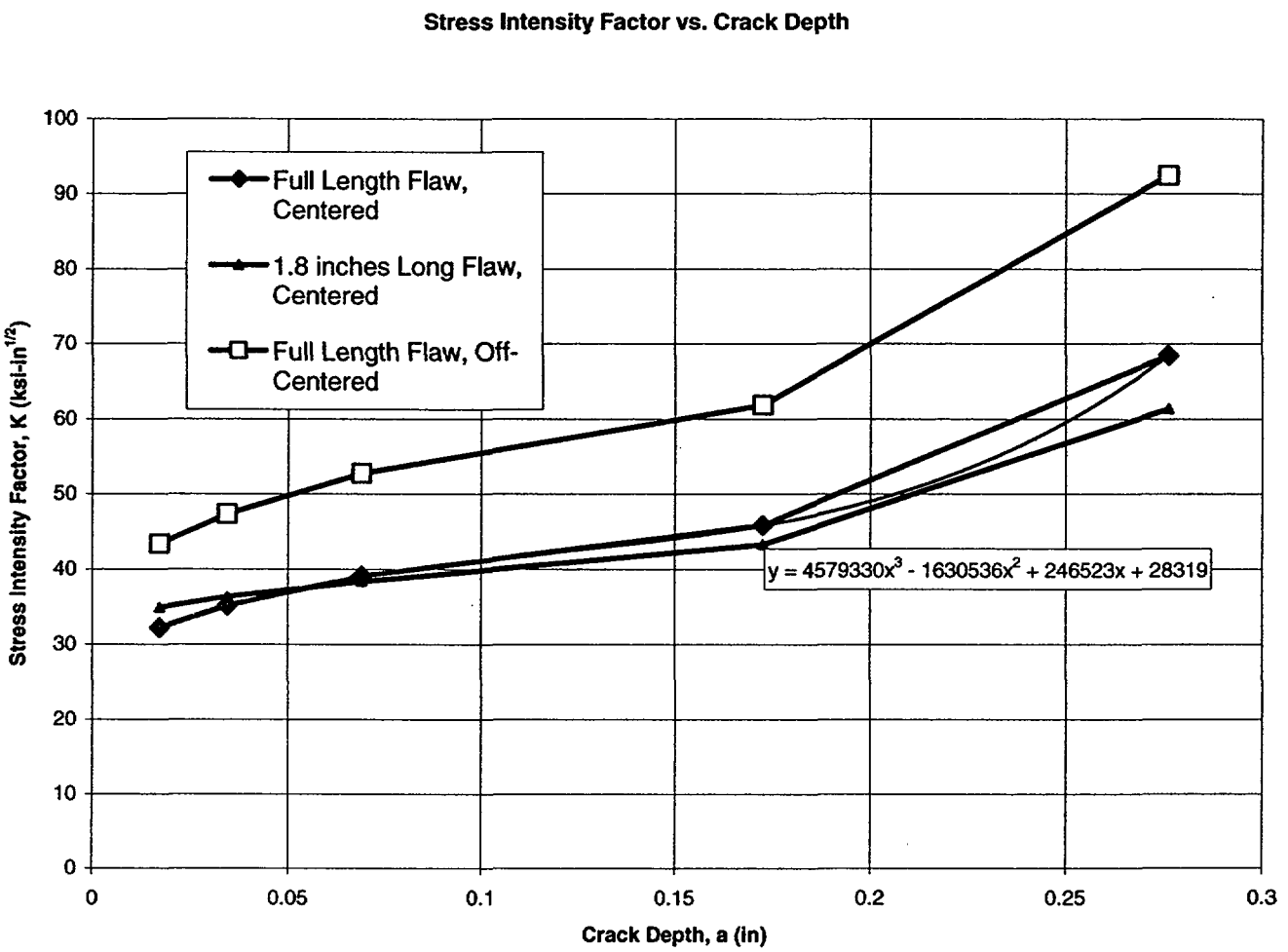

Figure 14: Maximum *K* versus *a*

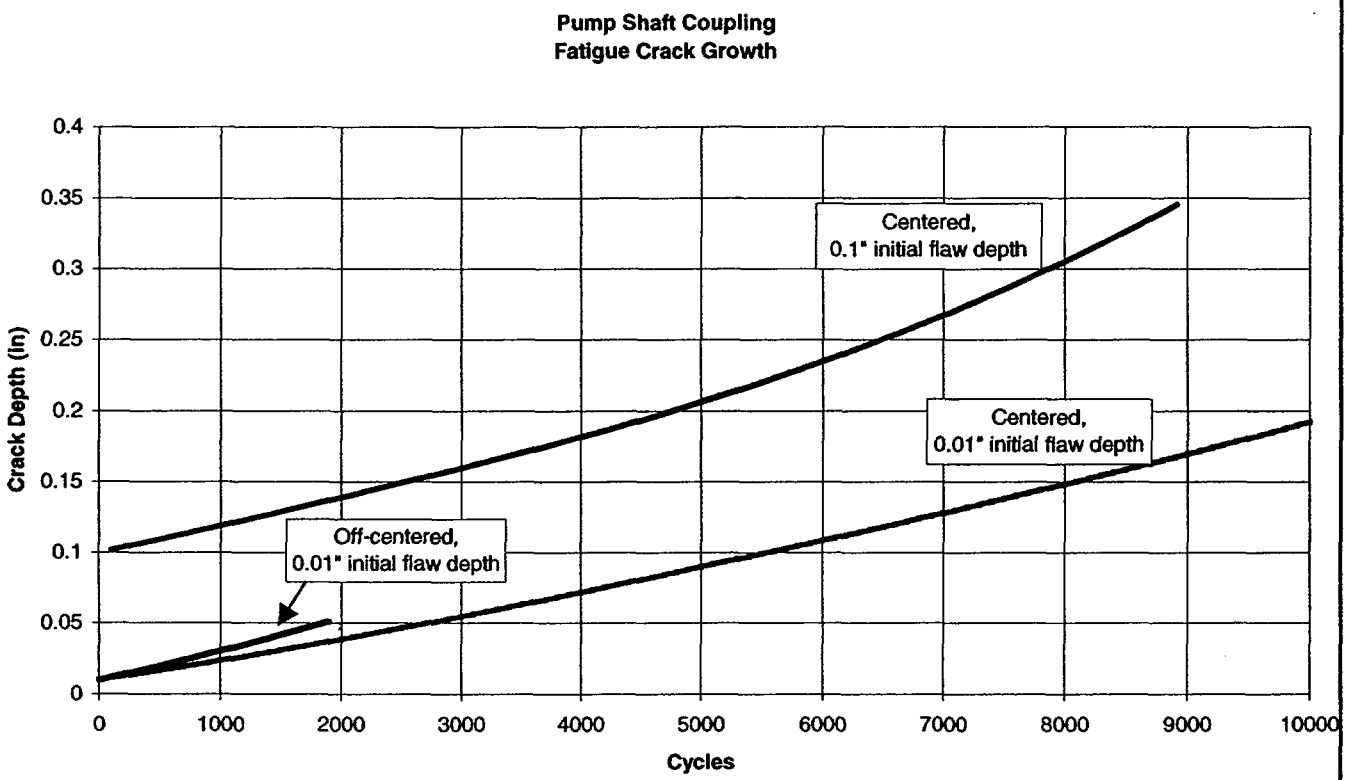

Figure 15: Fatigue Crack Growth Results

APPENDIX A

ANALYSIS INPUT AND OUTPUT FILES DESCRIPTION

ANSYS INPUT FILES

Input File	Description
FINE_CENTER.INP	Refined Finite element model geometry for the properly centered coupling
FM_MODEL.INP	File to create singular crack tip elements
LEFM_05.INP	Analysis file for the 5% crack depth case
LEFM_10.INP	Analysis file for the 10% crack depth case
LEFM_20.INP	Analysis file for the 20% crack depth case
LEFM_50.INP	Analysis file for the 50% crack depth case
LEFM_80.INP	Analysis file for the 80% crack depth case
KCALC_PERY.INP	Post-processing file to extract K results

ANSYS OUTPUT FILES

Output File	Description
POST_05.INP	K calculation routine output file for 5% crack depth case
POST _10.INP	K calculation routine output file for 10% crack depth case
POST _20.INP	K calculation routine output file for 20% crack depth case
POST _50.INP	K calculation routine output file for 50% crack depth case
POST _80.INP	K calculation routine output file for 80% crack depth case
K_05.CSV	K results output file for 5% crack depth case
K _10. CSV	K results output file for 10% crack depth case
K _20. CSV	K results output file for 20% crack depth case
K _50. CSV	K results output file for 50% crack depth case
K _80. CSV	K results output file for 80% crack depth case
K_Perry.xls	Excel spreadsheet for plotting and curve fitting K data

pc-CRACK™ INPUT FILES

Input File	Description
FAT_0001.LFM	Fatigue Crack Growth Analysis, Initial Depth = 0.001"
FAT_0005.LFM	Fatigue Crack Growth Analysis, Initial Depth = 0.005"
FAT_001.LFM	Fatigue Crack Growth Analysis, Initial Depth = 0.01"
FAT_005.LFM	Fatigue Crack Growth Analysis, Initial Depth = 0.05"
FAT_01.LFM	Fatigue Crack Growth Analysis, Initial Depth = 0.1"

pc-CRACK™ OUTPUT FILES

Output File	Description
FAT_0001.OUT	Fatigue Crack Growth Analysis Results, Initial Depth = 0.001"
FAT_0005.OUT	Fatigue Crack Growth Analysis Results, Initial Depth = 0.005"
FAT_001.OUT	Fatigue Crack Growth Analysis Results, Initial Depth = 0.01"
FAT_005.OUT	Fatigue Crack Growth Analysis Results, Initial Depth = 0.05"
FAT_01.OUT	Fatigue Crack Growth Analysis Results, Initial Depth = 0.1"

EXCEL SPREADSHEET

CRACK_GROWTH.XLS	Excel Spreadsheet for Curve Fitting Fatigue Crack Growth Rates and Plotting the Fatigue Analysis Results